PAPER • OPEN ACCESS

Macroscopic quantumness of optically conditioned mechanical systems

To cite this article: Hannah McAleese and Mauro Paternostro 2020 *New J. Phys.* **22** 093075

View the article online for updates and enhancements.

New Journal of Physics

The open access journal at the forefront of physics

CrossMark

PAPER

Macroscopic quantumness of optically conditioned mechanical systems

Hannah McAleese[*] and Mauro Paternostro

Centre for Theoretical Atomic, Molecular and Optical Physics, School of Mathematics and Physics, Queen's University, Belfast BT7 1NN, United Kingdom

[*] Author to whom any correspondence should be addressed.

E-mail: hmcaleese02@qub.ac.uk

Abstract

We address the macroscopic quantumness of the state of mechanical systems subjected to conditional protocols devised for state engineering in cavity optomechanics. We use a measure of macroscopicity based on phase-space methods. We cover the transition regime into strong single-photon coupling, illustrating how measurements performed over the cavity field that drives the dynamics of a mechanical system are able to steer the latter toward large quantum coherent states. The effect of losses is evaluated for the case of an open cavity and analyzed in terms of the features of the Wigner functions of the state of the mechanical system. We also address the case of engineered phonon-subtracted mechanical systems, in full open-system configuration, demonstrating the existence of optimal working points for the sake of mesoscopic quantumness. Our study is relevant for and applicable to a broad range of settings, from clamped to levitated mechanical systems.

Ever since Schrodinger's famous thought experiment [1], the concept of quantum superpositions in macroscopic systems has led many, both inside and outside the scientific community, to reconsider our understanding of physical reality. There remain numerous open questions about how the size of a system is related to its ability to exhibit quantum behavior. Macroscopic quantum states can be used to bring us closer to answering these questions and to understanding more clearly the quantum–classical boundary [2]. In addition, states of this kind are valuable resources for quantum computation and quantum metrology [3].

The identification of successful strategies for the generation of such macroscopic quantum states is an active area of investigation. Promising avenues in this direction have been explored in the field of cavity optomechanics [4–10], owing to the possibility offered by such a platform to transfer the quantumness of the state of a light field driving the motion of a mechanical system to the state of the latter [5]. The overarching scope of such endeavors is to take mesoscopic quantum states one step closer to experimental realization. This will allow the study of creation and decoherence of massive superpositions and thus will shed new light on the quantum–classical transition [6–8].

However, a currently open question is whether it is possible to define a comprehensive figure of merit able to *quantify* the degree of macroscopic quantumness of a given state. A range of measures of macroscopic quantumness have been proposed [11–28], based on different definitions and means of quantifying this concept. Such measures vary in regard to the physical systems to which they can be applied, the states for which they are relevant, and the features that characterise a given macroscopically quantum state.

In this paper, we focus on an optomechanical setting for the engineering of macroscopic quantum states and make use of the measure proposed in reference [19]. Such a phase-space based quantifier is instrumental to our purposes in light of the possibility to apply it to a broad range of both pure and mixed states of a mechanical system. With this choice of system and quantifier of macroscopic quantumness in mind, we investigate a scheme for the preparation of mesoscopic quantum states of a mechanical system

that is assisted by measurements performed on the optical field that drives the mechanical motion. We study the impact that measurements have on the resulting degree of mechanical macroscopicity, analyzing the influences of the specific measurement settings on the resultant mechanical state. We then use the results of such analysis to find effective measurement strategies to engineer mechanical states with enhanced degrees of macroscopicity. In this regard, we go significantly beyond the limitations of earlier assessments such as the one reported in references [9, 10]: we address quantitatively the detrimental effect of noise, search for the best-performing Gaussian measurement when gauged against the degree of macroscopicity of the conditional mechanical state, and characterise this state's features thoroughly, putting it in relation to a paradigmatic mesoscopically quantum state. Moreover, we explore the possibility to achieve macroscopic quantumness through the subtraction of photons from the field driving the mechanical motion, which embodies a novel avenue in the context addressed by our study.

The remainder of this paper is organized as follows. In section 1 we describe the systems that we consider. We then give in section 2 an introduction to the measure of macroscopic quantumness used to characterize the performance of the schemes that we analyze. In section 3 we illustrate the effect of conditional strategies on the state of the mechanical system and quantify the degree of macroscopic quantumness of the latter when performing either homodyne or heterodyne optical measurements, seeking for the optimal measurement strategy for the sake of macroscopicity. Section 4 is dedicated to the analysis of the effect of cavity damping on the degree of macroscopicity achieved through such a scheme. Section 5 illustrates an alternative approach to the establishment of mechanical macroscopic quantumness based on photon subtraction. Finally, in section 6 we provide our concluding remarks, while part of our formal analysis is reported in a technical appendix.

1. Optomechanical systems

We consider an optomechanical system in the standard dispersive-coupling regime described by the Hamiltonian [5]

$$H = \hbar\omega_o a^\dagger a + \hbar\omega_m b^\dagger b - \hbar g a^\dagger a (b + b^\dagger),
\tag{1}$$

where ω_o (ω_m) is the frequency of the cavity field (mechanical mode) whose annihilation and creation operators are a and $a^\dagger$ (b and $b^\dagger$). The rate $g = (\omega_o/L)\sqrt{\hbar/(2m\omega_m)}$ quantifies the vacuum optomechanical coupling strength. Here L is the length of the cavity and m is the effective mass of the mechanical oscillator. Under suitable conditions, such model embodies the Hamiltonian of systems as diverse as a single-sided cavity endowed with a clamped mechanical nanostructure and a levitated nanoparticle trapped in a cavity. For a consideration of systems with the linearised interaction Hamiltonian, see appendix A.

Throughout this manuscript, we assume the validity of the single-photon optomechanics, i.e. the regime where g exceeds the rate of losses within the system, which are typically set by the linewidth of the cavity. This regime also allows for the retention of the cubic form of the interaction in equation (1), which is a key feature of our scheme for the preparation of non-classical mechanical states. We emphasize that such interesting dynamical regime has not yet been achieved experimentally, but significant progress toward such operational conditions has been made. Reference [29] uses superconducting circuit-based optomechanics, where Josephson tunnel junctions make up a two-level system that couples the cavity and mechanical oscillator. The addition of this qubit enables much stronger coupling rates. In fact, the best coupling rate-to-linewidth ratio that has been reported reaches values as large as 0.01 [29]. Further theoretical calculations predict that the control of parameter values such as external magnetic flux and gate voltage of the device, one can achieve an increase in radiation-pressure coupling by up to two orders of magnitude [29]. Another promising avenue is the setting of optomechanical crystals [30], which limits thermal mechanical noise and increases the coupling strength. For instance, reference [30] reports on a silicon device with two one-dimensional (1D) nano-beam cavities coupled optically to a waveguide to achieve a coupling rate-to-linewidth ratio of the order of 10^{-3}. The use of quasi-2D devices could further improve such system and achieve even stronger rates. Our work thus paves the way to investigations addressing the next generation of optomechanical devices.

The time evolution operator corresponding to the Hamiltonian in equation (1) can be rearranged as

$$U(\tau) = e^{-ib^\dagger b\tau}\, e^{-ira^\dagger a\tau}\, e^{ik^2(a^\dagger a)^2[\tau - \sin(\tau)]} D_m(k\eta a^\dagger a),
\tag{2}$$

where the relevant parameters have been rescaled and cast in a dimensionless form as $r = \omega_o/\omega_m$, $k = g/\omega_m$ and $\tau = \omega_m t$ with t the evolution of the system. The term η relates to the dimensionless evolution time as $\eta = 1 - e^{-i\tau}$. We have introduced the displacement operator $D_m(x) = \exp[xb^\dagger - x^*b]$, which displaces the state of the mechanical mode in the phase space. Notice that the amplitude of the displacement performed

in equation (2) depends on the number of excitations in the state of the cavity field through the number operator $a^\dagger a$.

As in reference [5], we take the initial state of the cavity field and mirror to be coherent states $|\alpha\rangle_c$ and $|\beta\rangle_m$. This can be achieved by feeding the cavity with an input pump at frequency ω_p. We call $\Delta = \omega_o - \omega_p$ the detuning between pump and cavity field. For a resonant coupling between cavity field and external pump (i.e. for $\Delta = 0$), the state of the cavity mode is asymptotically driven to a coherent state of amplitude determined by the intensity of the pump. As for the mechanical system, coherent states can be engineered with large purity using pulsed-driving schemes as in references [31, 32]. For this initial preparation, the time-evolved state of the system is

$$|\psi(\tau)\rangle = e^{-|\alpha|^2/2}\sum_{n=0}^{\infty} c_n(\alpha, \tau)|n\rangle_c|\phi_n(\tau)\rangle_m, \tag{3}$$

where $\{|n\rangle_c\}$ are number states of the cavity field, $|\phi_n(\tau)\rangle_m$ is a coherent state of the mechanical system with amplitude $\phi_n(\tau) = k\eta n + \beta e^{-i\tau}$ and we have introduced the coefficients

$$c_n(\alpha, \tau) = \frac{(\alpha e^{\varphi})^n}{\sqrt{n!}} e^{ik^2 n^2[\tau - \sin(\tau)] - ir\tau n} \tag{4}$$

with $\varphi = k(\eta\beta^* e^{i\tau} - \eta^*\beta e^{-i\tau})/2$. As the displacement of the mechanical mode depends on the number of photons in the cavity, equation (3) describes, in general, an inseparable state.

2. Measure of macroscopic quantumness

We now briefly review the measure of macroscopic quantumness that has been used in our quantitative assessment. Following reference [19], we consider the quantity

$$\mathcal{I}(\rho) = \frac{1}{2\pi}\int (|\gamma|^2 - 1)|\chi(\gamma)|^2 \, d^2\gamma \tag{5}$$

where ρ is the density matrix of the system at hand, $\chi(\gamma) = \mathrm{Tr}[\rho D(\gamma)]$ is the Weyl characteristic function of state ρ [33], $\gamma \in \mathbb{C}$ is a phase-space variable. The first term in the integral (depending on $|\gamma|^2$) quantifies the magnitude of phase-space interference fringes that result from the possible quantum coherence inherent in the state of the system. The square modulus of the characteristic function, on the other hand, measures the frequency of such fringes and thus the size of the superposition state at hand [34]. Equation (5) thus allows us to quantify the degree of quantum coherence and size of the system simultaneously. Moreover, at variance with other quantifiers that have been recently proposed to determine the degree of macroscopicity of a quantum state, such quantity can be evaluated without the need for difficult optimization or special decompositions of the state ρ under scrutiny. As $\mathcal{I}(\rho)$ is based on the phase-space features of a state, it is well suited to address the macroscopic quantumness of bosonic systems and, in general, all those systems whose phase-space behavior is readily available. The maximum value that $\mathcal{I}(\rho)$ can take is the average number of particles or excitations in the state of the system N_ρ. Such upper bound is achievable only by pure states, mixed ones giving $\mathcal{I}(\rho) < N_\rho$, strictly [34]. As we are interested in characterizing the macroscopic quantumness of the mechanical system, in the remainder of this work we shall take $N_\rho = \langle b^\dagger b\rangle$.

An equivalent definition of $\mathcal{I}(\rho)$ reads [19]

$$\mathcal{I}(\rho) = -\frac{\pi}{2}\int W(\delta)\left(\frac{\partial^2}{\partial\delta\,\partial\delta^*} + 1\right)W(\delta)d^2\delta, \tag{6}$$

where we have introduced the Wigner function of a single harmonic oscillator

$$W(\delta) = \frac{1}{\pi^2}\int e^{\gamma^*\delta - \gamma\delta^*}\chi(\gamma)d^2\gamma \tag{7}$$

with $\delta \in \mathbb{C}$. Equation (7) suggests that schemes for the reconstruction of $W(\delta)$ would provide an avenue to the quantification of the degree of macroscopic quantumness of the mechanical state. For instance, following the implementation reported in reference [35], we could consider an additional optical field that, after the preparation of a given state of the mechanical system, allows for the reconstruction of its Wigner function. Needless to say, the data acquired through such method would have to be de-convoluted from the noise induced at the detection stage and which might hinder the non-classicality entailed by a negative Wigner function.

Finally, it is also interesting to note that this measure of macroscopic quantumness corresponds to a measure of the fragility of the system subjected to the effects of the environment it is coupled to [19]. If we model losses of this system through the Lindblad master equation

$$\frac{d\rho}{dt} = \mathcal{L}(\rho) = a\rho a^{\dagger} - \frac{1}{2}\{\rho, a^{\dagger}a\}, \tag{8}$$

then we can express $\mathcal{I}(\rho)$ in terms of the susceptibility of the state of the system to lose purity when subject to such process as [19]

$$\frac{d\mathcal{P}(\rho)}{dt} = -2\mathcal{I}(\rho), \tag{9}$$

where $\mathcal{P}(\rho) = \mathrm{Tr}(\rho^2)$ is the purity of state ρ. In this way, the measure of macroscopic quantumness that we use not only quantifies size and quantum coherence but also relates to robustness properties of macroscopic superpositions against specific classes of decoherence processes.

3. Conditioning the state of the mechanical system

Equation (3) shows that the reduced state of the mechanical oscillator consists of a convex sum of coherent states, which will then exhibit no quantum feature. However, the entanglement that is in general shared by cavity field and mechanical system allows to condition the state of the latter by means of controlled quantum operations on the former. In particular, the performance of projective measurements onto the state of the cavity field provides a powerful tool for the achievement of potentially interesting states of the mechanical system, when gauged against their degree of non-classicality [5, 9].

In order to generate a quantum state of the mirror, we thus need to subject the field to a measurement that results in the superposition of the coherent states that appear in equation (3). This rules out photon-counting as a suitable strategy to implement in light of the form of the joint optomechanical states. We thus resort to general-dyne measurements encompassing Gaussian measurements, which can be modeled as von Neumann projections of the cavity field onto suitable Gaussian states [33]. We define ideal homodyne and heterodyne measurements as measurements made using photodetectors with unit efficiency.

In particular, ideal homodyning along arbitrary directions in phase space implies the projection onto the eigenstates $|x(\theta)\rangle$ of the quadrature $x(\theta) = ae^{i\theta} + \text{h.c.}$, i.e.

$$|x(\theta)\rangle = e^{-x^2/2}\sum_{n=0}^{\infty}\frac{e^{i\theta n}}{\sqrt{2^n n!}\pi^{1/4}}H_n(x)|n\rangle \tag{10}$$

with $H_n(x)$ the Hermite polynomials of order n and variable $x \in [-\infty, \infty]$ and $\theta \in [0, 2\pi]$ a phase-space angle. As for ideal heterodyne, they are *de facto* modeled as projections onto coherent states $|\sigma\rangle$ with $\sigma \in \mathbb{C}$ [36]. In what follows, we will use the notation $M = \text{hom}$ ($M = \text{het}$) to indicate a homodyne (heterodyne) measurement.

Regardless of the specific form of the measurement being implemented, the conditional state of the mechanical mode (after normalization) can be cast in the general form

$$|\psi'\rangle_{\mathrm{m}} = \mathcal{N}_M \, e^{-|\alpha|^2/2}\sum_{n=0}^{\infty}d_n(\alpha, \tau)|\phi_n(\tau)\rangle_{\mathrm{m}} \tag{11}$$

with $\mathcal{N}_M$ a measurement-dependent normalization constant whose form is immaterial, and $d_n(\alpha, \tau) = c_n(\alpha, \tau)f_M(n)$, where

$$f_M(n) = \begin{cases} \dfrac{1}{\sqrt{n!}} e^{-|\sigma|^2/2}\sigma^{*n} & \text{for } M = \text{het},\\[2ex] \dfrac{1}{\sqrt{2^n n!}\sqrt[4]{\pi}} e^{-x^2/2 - i\theta n}H_n(x) & \text{for } M = \text{hom}. \end{cases} \tag{12}$$

In turn, the characteristic function of such conditional states can be written in a general fashion as

$$\chi(\gamma) = \mathcal{N}_M^2 \sum_{n,l=0}^{\infty} e^{-|\alpha|^2}\mathcal{M}_{n,l}(\alpha, \tau)\mathcal{F}_{n,l}(\gamma, \tau) \tag{13}$$

with $\mathcal{M}_{n,l}(\alpha,\tau) = d_n(\alpha,\tau)d_l^*(\alpha,\tau)$, which is fully determined by the choice of measurement being performed, and $\mathcal{F}_{n,l}(\alpha,\tau)$ the *universal* (i.e. measurement independent) function.

$$\mathcal{F}_{n,l}(\gamma,\tau) = {}_{\mathrm{m}}\langle\phi_l(\tau)|D(\gamma)|\phi_n(\tau)\rangle_{\mathrm{m}}$$

$$= \mathrm{e}^{-(|\phi_l(\tau)|^2 + |\gamma+\phi_n(\tau)|^2)/2 + \gamma\phi_n^*(\tau) - \gamma^*\phi_l(\tau)}. \tag{14}$$

As this is the only γ-dependent part of the characteristic function, it is the only term contributing to the phase-space integral inherent in the definition of the measure of macroscopic quantumness. We shall thus consider the integral

$$\int (|\gamma|^2 - 1)\mathcal{F}_{n,l}(\gamma,\tau)\mathcal{F}_{p,q}^*(\gamma,\tau)\mathrm{d}^2\gamma$$

$$= \pi[\phi_l(\tau) - \phi_p(\tau)]^*[\phi_q(\tau) - \phi_n(\tau)]\mathrm{e}^{\phi_l^*(\tau)\phi_q(\tau) + \phi_n(\tau)\phi_p^*(\tau) - \frac{1}{2}\sum\limits_{j=l,n,p}|\phi_j(\tau)|^2}, \tag{15}$$

which would enter equation (5) to account for the contribution arising from the superposition of coherent states in equation (11).

3.1. Effect of homodyne detection

With this result at hand, we can now evaluate measure $\mathcal{I}$ for different choices of the measurement strategy. Motivated by reference [5], we shall start considering the case of ideal and general homodyne measurements of the field, aiming at identifying the role played by the phase-space angle θ, the *effective interaction strength* k and the value $x(\theta)$ of the homodyne signal.

In figure 1(a) we address the effect that a growing value of k has on the measure of macroscopicity for various choices of the phase-space angle θ and for a homodyne measurement with postselection of the $x = 0$ outcome. Only at small values of k is the angle θ relevant in the determination of the degree of macroscopicity. However, there is no clear hierarchy among the values of $\mathcal{I}$ associated with a growing θ as the curves corresponding to different choices of the phase space angle are very intertwined and cross each other at multiple points. As k grows, such curves tend toward a monotonic behavior with virtually no dependence on the specific choice of θ made for the measurement setting. The region of large values of the effective interaction strength also corresponds to a shrinking gap with the mean number of excitations in the mechanical mode $\langle b^\dagger b\rangle$, thus providing evidence of a stronger macroscopically quantum behavior of the conditional state of the mechanical mode. The relation among the trends followed for the various choices of values of θ considered in our study is found also in the behavior of the mean number of excitations, thus showing that $\mathcal{I}$ is able to capture—in a faithful manner—intrinsic features of the states we have been considering. These considerations are found to hold also for $x \neq 0$, as shown in the example provided by the inset of figure 1(a), which is for $x = 1$. While non-zero values of x deliver the same qualitative results as for $x = 0$, the value of k starting from which any dependence on θ is apparent is larger for $x \neq 0$ than for projections onto the origin of the phase space. Moreover, the value of k at which $\mathcal{I} \simeq \langle b^\dagger b\rangle$ appears to bear a dependence on the choice of x.

In order to investigate further the influence that various choices of θ and x have on the degree of macroscopicity, we now fix the value of k. As a compromise between the size of our computation and the degree of macroscopicity that we aim at achieving, in what follows and unless otherwise specified, we consider $k = 1$, which corresponds to a sizable macroscopic superposition and a working point where the dependence on θ is less complex than for lower values of such parameter. Figure 1(b) shows that, as x grows, a non-zero value of θ is detrimental to the degree of macroscopicity being achieved through homodyne measurements, although the variations in $\mathcal{I}$ are small. This suggests that, regardless of the value of the homodyne signal being post-selected, the best strategy is to project onto eigenstates of the position quadrature. This is further illustrated in figure 2(a), where we study the relation between $\mathcal{I}$ and the mean number of bosonic excitations against x and for a few values of θ, showing the general decreasing trend of the degree of macroscopicity with a growing phase-space angle and the existence of a θ-independent value of the homodyne signal $\bar{x} = 1.427\,01$ at which $\mathcal{I} \simeq \langle b^\dagger b\rangle$. We shall call $\mathcal{I}_{\mathrm{opt}}$ the degree of macroscopicity at this value of $\bar{x}$. Figure 2(b) shows that $\mathcal{I}_{\mathrm{opt}}$ follows an approximatively sinusoidal trend.

Having identified a potentially optimal working point for the case of homodyne measurements, we now aim at characterizing the state of the mechanical mode achieved correspondingly. To this goal, we focus on the Wigner function of the mechanical mode at $x = \bar{x}$, $\theta = 0$ and the parameters used in figure 1 (which are motivated by the analysis reported in reference [5]). Figure 3(a) shows significant quantum coherence in the state of the mechanical mode, as witnessed by the large interference fringes (taking both positive and negative values) between two symmetrically placed Gaussian distributions. These features, which are
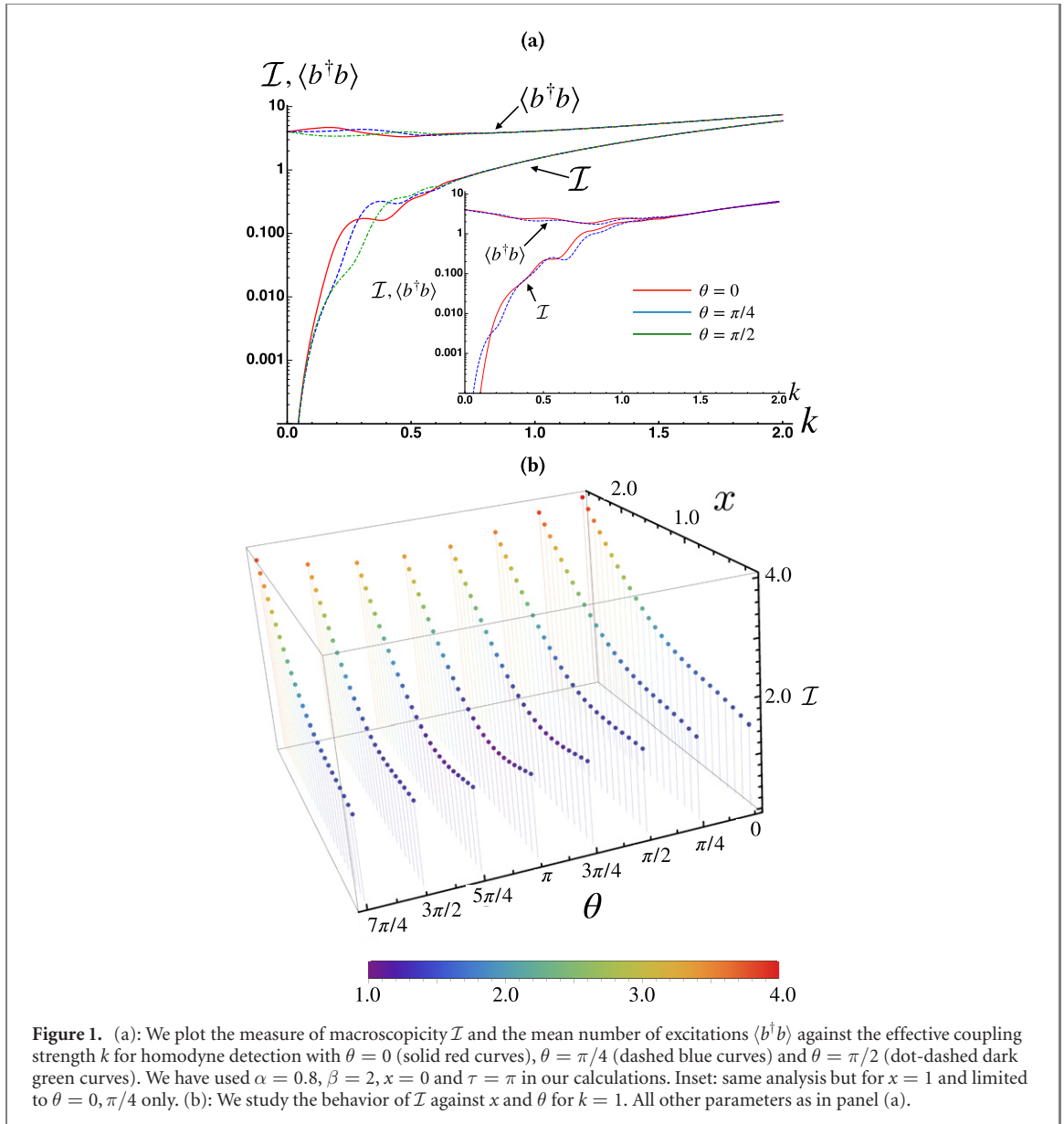
Figure 1. (a): We plot the measure of macroscopicity $\mathcal{I}$ and the mean number of excitations $\langle b^\dagger b \rangle$ against the effective coupling strength k for homodyne detection with $\theta = 0$ (solid red curves), $\theta = \pi/4$ (dashed blue curves) and $\theta = \pi/2$ (dot-dashed dark green curves). We have used $\alpha = 0.8$, $\beta = 2$, $x = 0$ and $\tau = \pi$ in our calculations. Inset: same analysis but for $x = 1$ and limited to $\theta = 0, \pi/4$ only. (b): We study the behavior of $\mathcal{I}$ against x and θ for $k = 1$. All other parameters as in panel (a).

reminiscent of those of a Schrödinger cat state having the form of a quantum superposition of coherent states—a similarity that we will address quantitatively later on in this paper—account for the macroscopically quantum character witnessed by $\mathcal{I}$. The analysis of the Wigner function allows us to gather an intuition of the depleted degree of macroscopic quantumness resulting from non-zero values of θ. In figures. 3(b) and (c) we report $W(\delta)$ for $\theta = \pi/4$ and $\pi/2$ respectively, showing that the symmetry that is characteristic of the case with $\theta = 0$ is lost. This suggests that the effect of θ is that of biasing the quantum superposition toward one component, thus strongly depleting the other one and justifying intuitively the decrease of $\mathcal{I}$ observed in figure 2(a).

In order to address the similarity of the mechanical mode state to a quantum superposition of displaced coherent states, we have considered the state fidelity $F = |\langle \mathrm{cat}(\lambda)|\psi'\rangle_\mathrm{m}|^2$ between the post-measurement state of the mechanical mode and the cat state $|\mathrm{cat}(\lambda)\rangle \propto |\lambda\rangle + |-\lambda\rangle$ with $|\pm\lambda\rangle$ two coherent states of opposite phase and amplitude $\lambda \in \mathbb{C}$ that we treat as an unknown parameter. Maximizing F with respect to the coherent state amplitude λ of the cat state for $x = \bar{x}$ and the values of the other parameters used in figure 3(a), we find a maximum of 0.592 for $\mathrm{Re}(\lambda) \simeq 0$ and $\mathrm{Im}(\lambda) = 0.715$. Such fidelity decreases to 0.5649 and 0.5646 for the parameters corresponding to the Wigner functions in figures 3(b) and (c) respectively.

While this result gives evidence of the decreased *cat-like* nature of states with non-zero θ, the value of F achieved for $\theta = 0$ is surprisingly low. However, a simple analysis allows us to interpret such result. We shall consider a simplified version of the conditional state of the mechanical mode consisting only of the most relevant components in equation (11). These are easily identified by looking at the coefficients
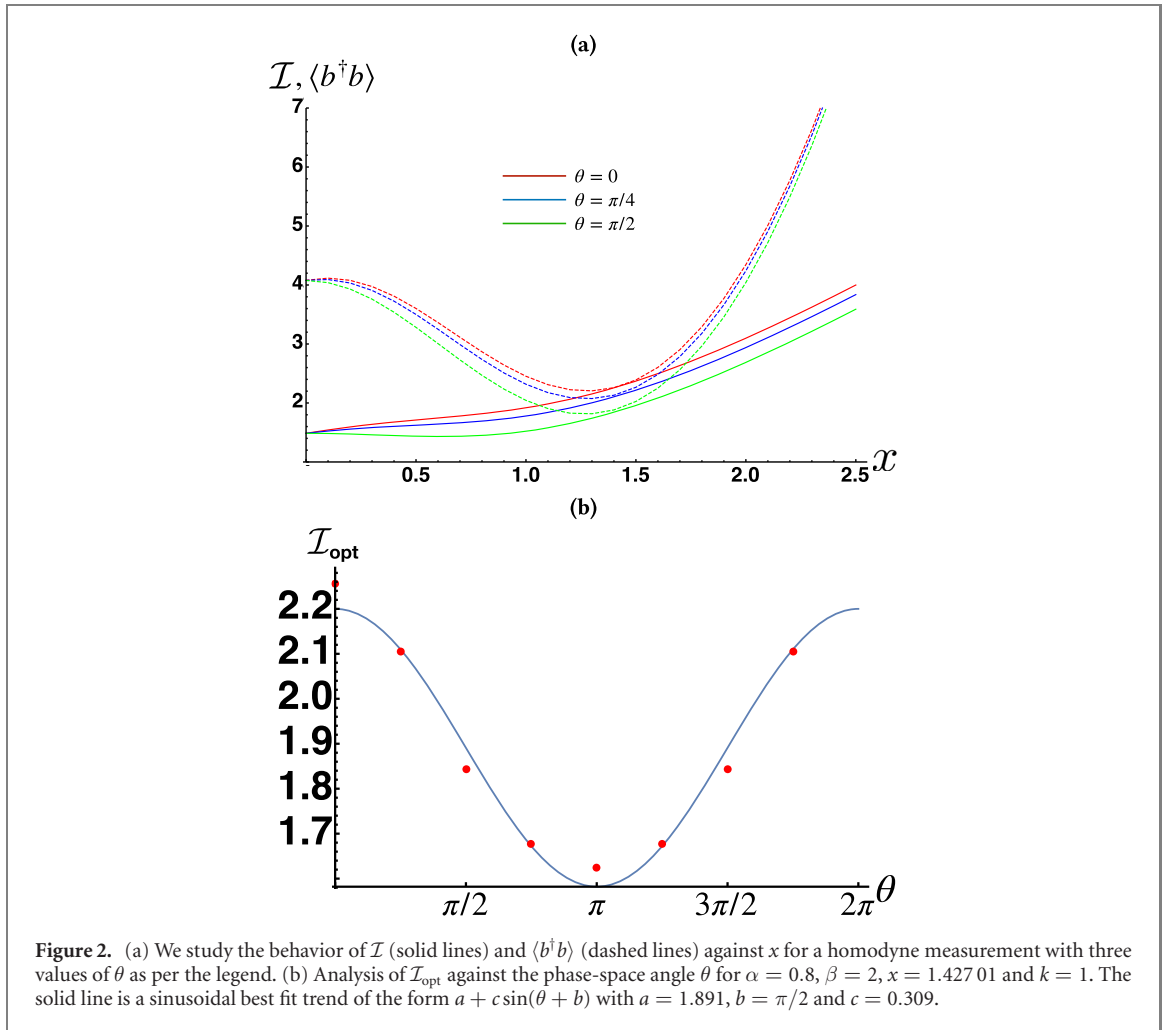
Figure 2. (a) We study the behavior of $\mathcal{I}$ (solid lines) and $\langle b^\dagger b \rangle$ (dashed lines) against x for a homodyne measurement with three values of θ as per the legend. (b) Analysis of $\mathcal{I}_{\mathrm{opt}}$ against the phase-space angle θ for $\alpha = 0.8$, $\beta = 2$, $x = 1.427\,01$ and $k = 1$. The solid line is a sinusoidal best fit trend of the form $a + c\sin(\theta + b)$ with $a = 1.891$, $b = \pi/2$ and $c = 0.309$.

$|\mathcal{N}_{\mathrm{hom}}\, \mathrm{e}^{-\alpha^2/2} d_n(\alpha, \tau)|^2$. Figure 4(a) shows them for $n = 0, \ldots, 10$, evidencing that all coefficients associated with $n \geqslant 3$ are in fact negligibly small. We can therefore consider state $|C\rangle$ made up of only three terms. Moreover, the value of the coefficient for $n = 1$ is much higher than the that of $n = 0$ and 2, which are roughly the same. We thus consider the simplified conditional state $|C\rangle_{\mathrm{m}}$ given by

$$|C\rangle_{\mathrm{m}} = \mathcal{N}'_{\mathrm{hom}} \left(d_0(\alpha, \tau)|\phi_0(\tau)\rangle_{\mathrm{m}} + d_2(\alpha, \tau)|\phi_2(\tau)\rangle_{\mathrm{m}} + \mu d_1(\alpha, \tau)|\phi_1(\tau)\rangle_{\mathrm{m}} \right) \tag{16}$$

with $\mathcal{N}'_{\mathrm{hom}}$ the normalization constant and μ a weight parameter that we add to gauge the effect that $|\phi_1(\tau)\rangle_{\mathrm{m}}$ has on the fidelity with a cat state. In particular, we look for the value that μ and λ should take in order for the fidelity to be maximum. Our numerical analysis shows that one should take $\mathrm{Im}[\lambda] = 0$ and reduce μ as much as possible in order to have a state fidelity close to 1 (cf figure 4(b)). It is thus clear that the non-ideal fidelity highlighted above is the result of the contribution given by $|\phi_1(\tau)\rangle_{\mathrm{m}}$ to the conditional state of the mechanical mode.

3.2. Effect of heterodyne detection

We have performed a similar analysis when, this time, the cavity field is subjected to ideal heterodyne measurements. As mentioned in section 3, these can be formally described as von Neumann projections onto coherent states of arbitrary amplitude $\sigma \in \mathbb{C}$, which deliver a conditional state of the mechanical mode reading

$$|\psi'\rangle_{\mathrm{m}} = \mathcal{N}_{\mathrm{het}}\, \mathrm{e}^{-|\alpha|^2/2} \sum_{n=0}^{\infty} c_n(\alpha, \tau) f_{\mathrm{het}}(n)|\phi_n(\tau)\rangle_{\mathrm{m}} \tag{17}$$

with $f_{\mathrm{het}}(n)$ as given in equation (12). Scope of the analysis reported here is not only to infer the effectiveness of this conditional scheme to generate macroscopic quantum superpositions of the state of the mechanical mode, but also to evaluate the relative performance with the scheme based on homodyning.

In figure 5 we report a summary of the results that we have gathered by considering increasing values of
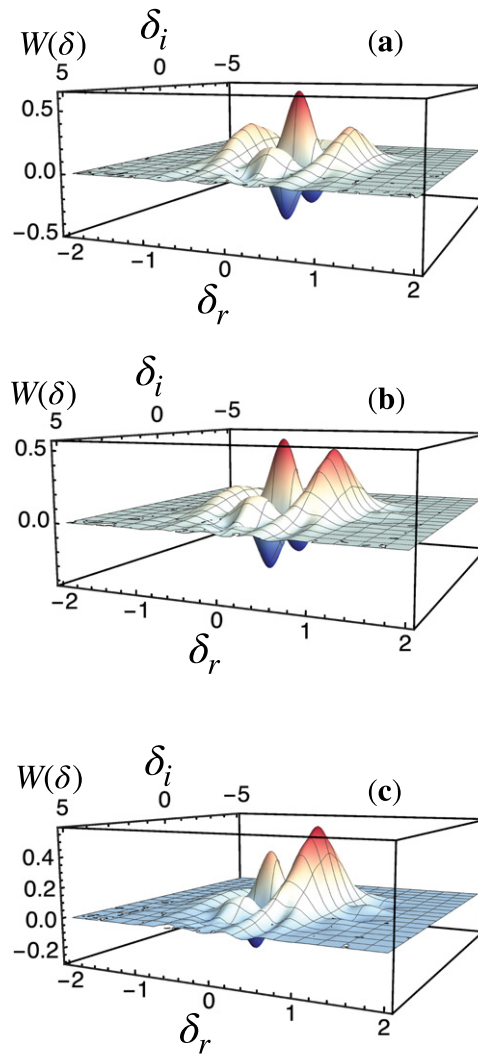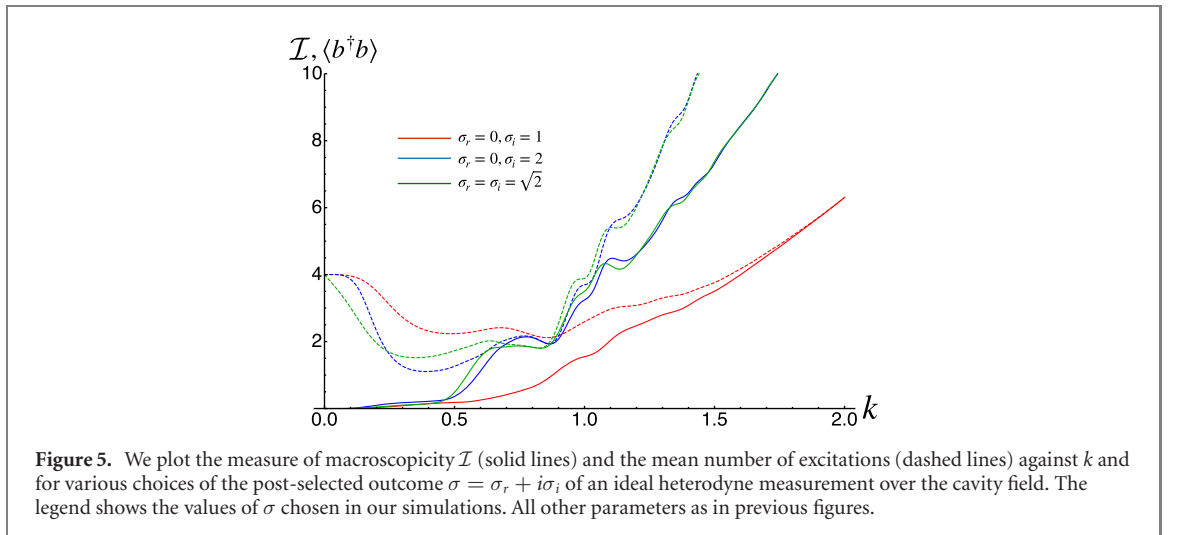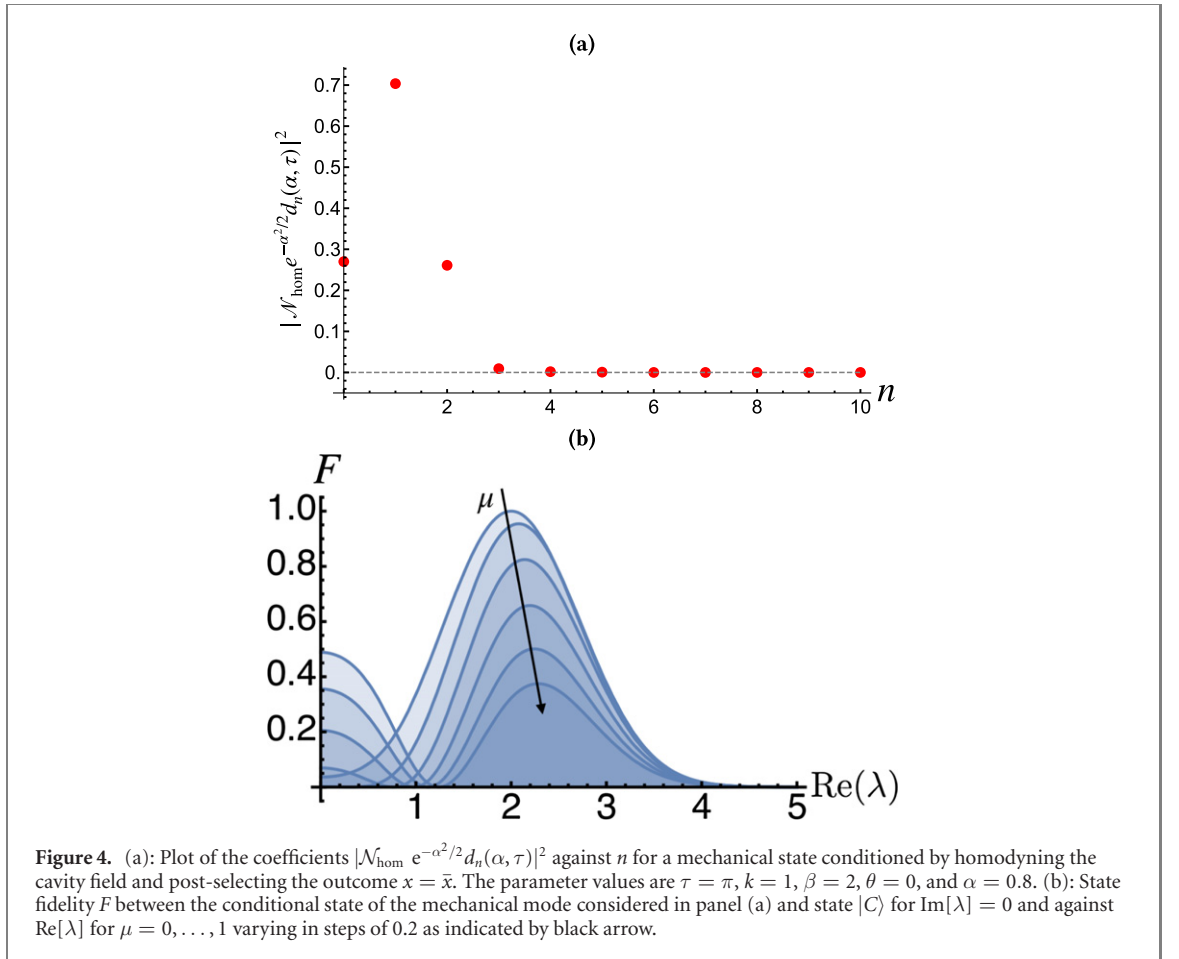
Figure 3. Wigner function of ρ_B when $x = 1.427\,01$. The Wigner function is reminiscent of that of a cat state, with interference between two positive states. In this case, the parameter values are $\alpha = 0.8$, $\beta = 2$, $k = 1$ and $\tau = \pi$.

the effective coupling strength k and various choices of the amplitude $\sigma = \sigma_r + i\sigma_i$. A first consideration to make is as follows: when looking at the same range of k as in figure 1(a), the value of $\mathcal{I}$ achieved for a homodyne measurement with $x = \theta = 0$ is comparable with what is found for a heterodyne measurement with $\sigma_r = 0, \sigma_i = 1$. We can thus say that projections onto $|x(0) = 0\rangle$ and $|\sigma = i\rangle$ embody comparable resources, as far as the degree of macroscopic quantumness is concerned. However, contrary to the homodyne-measurement case—where the gap between degree of macroscopicity and mean number of excitations remains wide for any $k \leqslant 2$, heterodyning returns states such that $\mathcal{I} \simeq \langle b^\dagger b \rangle$. In this sense, one can legitimately claim for the superiority of a strategy based on heterodyning.

Exploring further the phenomenology resulting from heterodyne measurements, one intuitively expects that larger values of $|\sigma|$ could lead to larger degrees of macroscopicity $\mathcal{I}$ in light of the linear dependence of equation (12) from σ^*. This appears to be the case, as highlighted in figure 5, where it is also shown that the degree of macroscopicity is strongly determined by the choice of $|\sigma|$ and not of its real and imaginary parts per se.

The calculation of the Wigner function associated with the state of the conditional mechanical oscillator for the three cases addressed in figure 5 leads to the distributions reported in figure 6, which are endowed with significant quantum coherences, as witnessed by the pronounced interference fringes in phase space. The different shapes taken by the Wigner functions as σ changes can be justified through the analysis of the distribution of coefficients $|\mathcal{N}_{\text{het}}\, \mathrm{e}^{-\alpha^2/2} d_n(\alpha, \tau)|^2$ against n: small values of $|\sigma|$ give rise to coefficients that are monotonically decreasing with n, so that the superposition in equation (11) is strongly biased toward $|\phi_0(\alpha, \tau)\rangle$. As $|\sigma|$ grows, a structure similar to the one shown in figure 4(a) emerges, leading to an increasing cat-like nature of the state of the mechanical mode. An analysis similar to the one performed

Figure 4. (a): Plot of the coefficients $|\mathcal{N}_{\text{hom}}\ e^{-\alpha^2/2}d_n(\alpha,\tau)|^2$ against n for a mechanical state conditioned by homodyning the cavity field and post-selecting the outcome $x = \bar{x}$. The parameter values are $\tau = \pi$, $k = 1$, $\beta = 2$, $\theta = 0$, and $\alpha = 0.8$. (b): State fidelity F between the conditional state of the mechanical mode considered in panel (a) and state $|C\rangle$ for $\text{Im}[\lambda] = 0$ and against $\text{Re}[\lambda]$ for $\mu = 0, \ldots, 1$ varying in steps of 0.2 as indicated by black arrow.

Figure 5. We plot the measure of macroscopicity $\mathcal{I}$ (solid lines) and the mean number of excitations (dashed lines) against k and for various choices of the post-selected outcome $\sigma = \sigma_r + i\sigma_i$ of an ideal heterodyne measurement over the cavity field. The legend shows the values of σ chosen in our simulations. All other parameters as in previous figures.

before for homodyne measurements shows that for $|\sigma| = 1.75$ the state of the mechanical oscillator can be very well approximated by the three-component superposition

$$|\psi'\rangle_{\text{m}} \simeq \mathcal{N}_{\text{het}}\ e^{-|\alpha|^2/2}\sum_{j=0}^{2}\left(d_j(\alpha,\tau)|\phi_j(\tau)\rangle_{\text{m}}\right) \qquad (18)$$

with $d_1(\tau)$ being purely imaginary and $d_0(\tau)$, $d_2(\tau) \in \mathbb{R}$ such that $|d_1(\tau)| \gg d_0(\tau) \simeq -d_2(\tau)$. The corresponding fidelity with a cat state of the form $|\lambda\rangle - |-\lambda\rangle$ is as large as 99.92% for $\lambda \simeq 2.003$.

Figure 6. We report the Wigner function associated with the state of the mechanical system for the three cases addressed in figure 5 and $k = 1$.
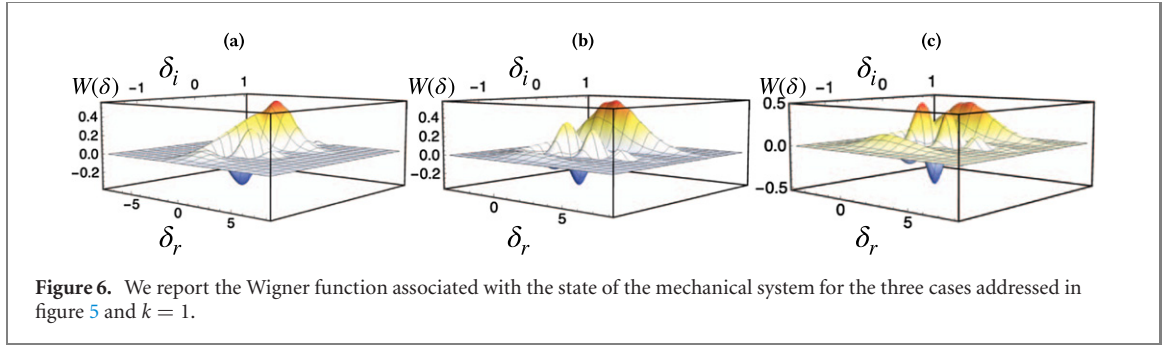
4. Effect of cavity dissipation on the degree of macroscopicity

We now address the effect that losses affecting the cavity have on the degree of macroscopicity of the mechanical mode, thus deviating from the unitary picture discussed so far. We shall restrict our attention to cavity dissipation, without worry about mechanical damping, as the latter typically occurs in timescales that are much longer than the decay of the cavity field owing to the large mechanical quality factors that can be achieved in current state-of-the-art optomechanical experiments. We thus model the open-system dynamics of the overall system through the master equation

$$\frac{d\rho}{dt} = -\frac{i}{\hbar}[H, \rho] + \frac{\kappa}{2}(2a\rho a^\dagger - \{a^\dagger a, \rho\}) \tag{19}$$

where κ is the decay rate of the cavity field and H is the Hamiltonian in equation (1) in the interaction picture.

Guided by the analysis performed in the previous Sections, we shall retain a value of the effective coupling strength of the order of $k \sim 1$. This entails that, in order to make our calculations accurate, we should retain values up to $n = 10$ in equation (3), thus making the direct solution of equation (19) a difficult problem. We thus resort to a quantum unraveling approach [37] based on the chopping of the time window within which we are interested in tracking the dynamics of the system in $n \gg 1$ small time steps $\delta\tau$. At the nth time step (such that $n\delta\tau = \tau$), we calculate the probability that a quantum jump of the state $|\psi(\tau)\rangle$ occurs, which is evaluated as

$$\delta p = \kappa\delta\tau\langle\psi(\tau)|a^\dagger a|\psi(\tau)\rangle. \tag{20}$$

Such probability is typically much less than 1. We then generate a random number $\epsilon \in [0, 1]$: should we have $\epsilon > \delta p$, the state of the system at time $\tau + \delta\tau$ becomes

$$|\psi(\tau + \delta\tau)\rangle = (\mathbb{1} - i\tilde{H}\delta\tau)|\psi(\tau)\rangle, \tag{21}$$
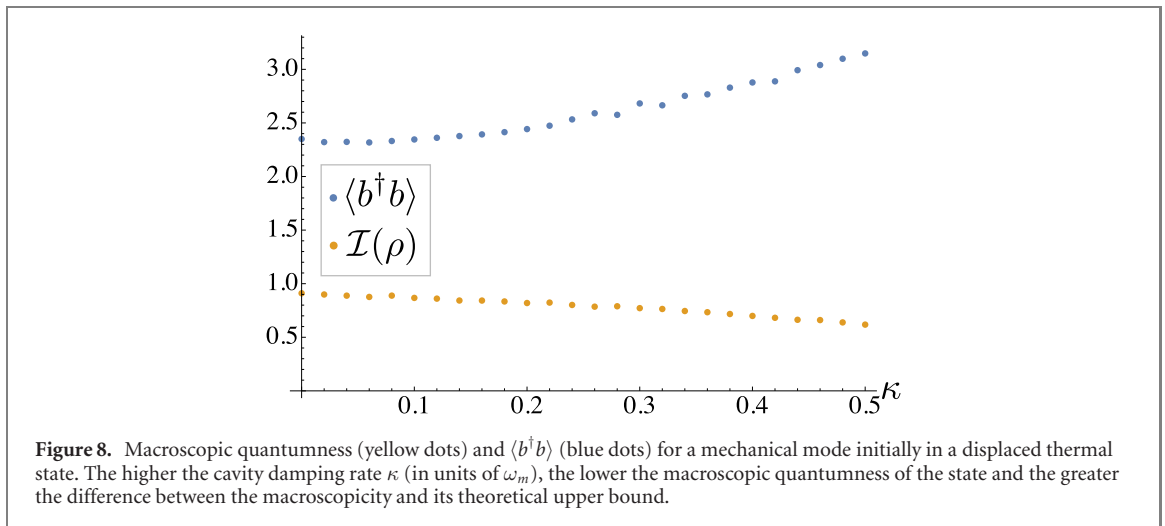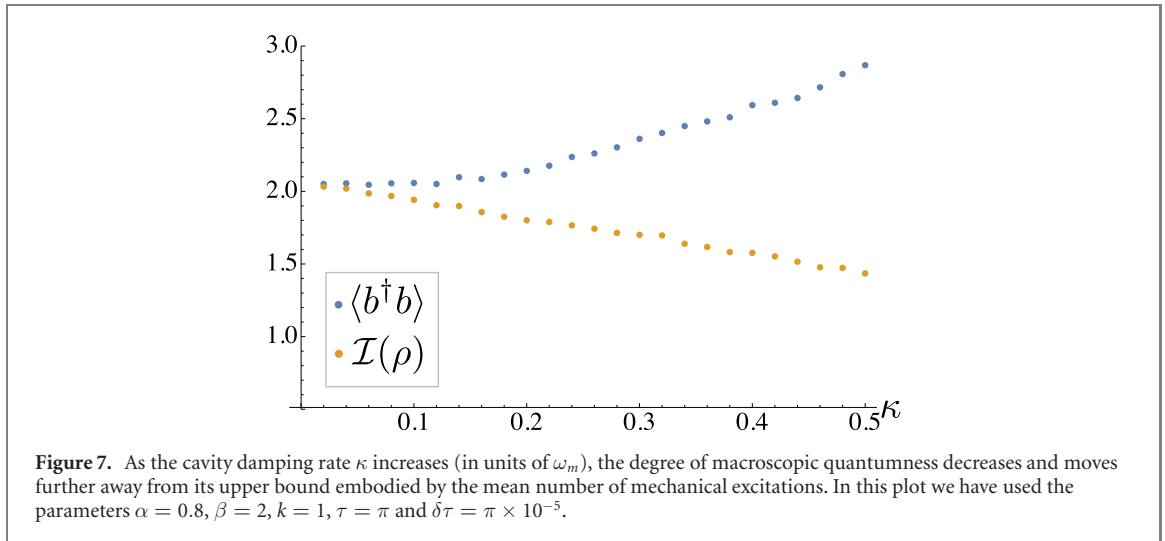
where $\tilde{H}$ is the non-Hermitian interaction-picture Hamiltonian

$$\tilde{H} = -ka^\dagger a(b\, e^{i\tau} + b^\dagger e^{-i\tau}) - i\kappa a^\dagger a. \tag{22}$$

In the less probable case of $\delta p > \epsilon t$, a quantum jump described by the operator $C = \sqrt{\kappa}a$ occurs, effectively leaking a photon of the cavity. This algorithm is repeated at every time step to achieve a dynamical trajectory. Many such trajectories are then constructed and the state of the system built as their ensemble average to remove any dependence over the realization of the sequence of quantum jumps.

The unraveling strategy is used to address the effect that a growing cavity decay rate has on the macroscopic nature of the conditional mechanical state achieved when performing homodyne measurements (no qualitative difference is found when heterodyne measurements are chosen). The results are reported in figure 7, where κ is measured in units of ω_m. The cavity dissipation evidently induces a decrease of the degree of macroscopicity achieved for $\kappa = 0$, $\theta = 0$ and the same parameters used in the simulations reported in figure 1. Moreover, we find a bifurcation between the mean number of excitations in the mechanical state and $\mathcal{I}(\rho)$: as the cavity damping rate increases, the state of the mechanical system becomes more mixed than in the unitary-dynamics case, thus magnifying the difference between the actual degree of macroscopicity and its maximum achievable value.

How does this result depend on the initial state of the mechanical system? In order to address this question we generalized the assumptions made in the previous Sections and consider the mechanical mode
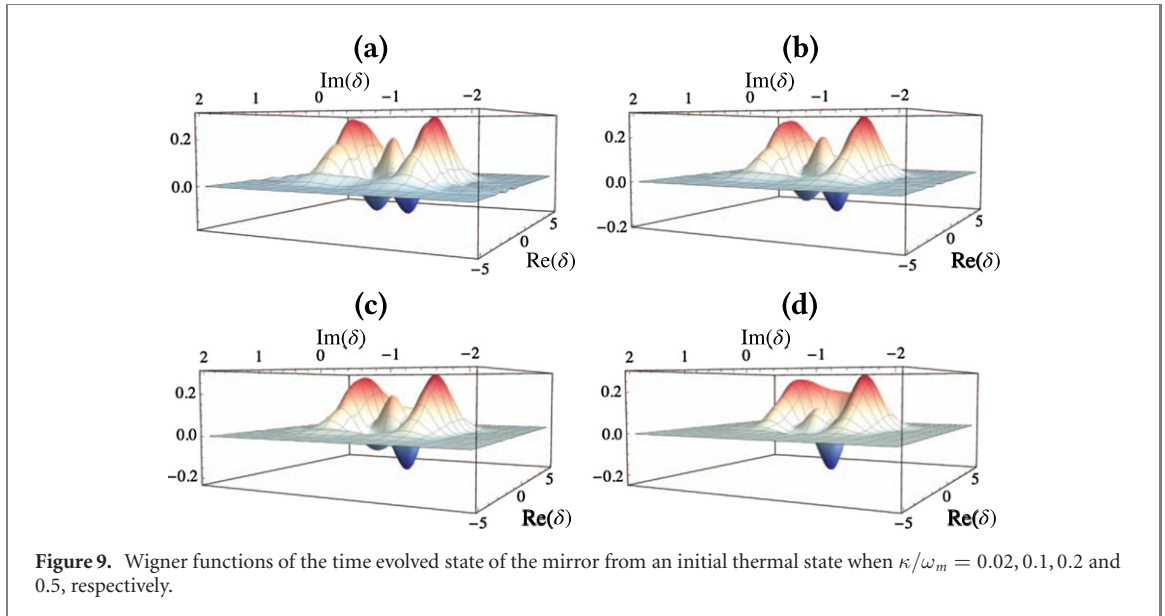
Figure 7. As the cavity damping rate κ increases (in units of ω_m), the degree of macroscopic quantumness decreases and moves further away from its upper bound embodied by the mean number of mechanical excitations. In this plot we have used the parameters $\alpha = 0.8, \beta = 2, k = 1, \tau = \pi$ and $\delta\tau = \pi \times 10^{-5}$.

Figure 8. Macroscopic quantumness (yellow dots) and $\langle b^\dagger b \rangle$ (blue dots) for a mechanical mode initially in a displaced thermal state. The higher the cavity damping rate κ (in units of ω_m), the lower the macroscopic quantumness of the state and the greater the difference between the macroscopicity and its theoretical upper bound.

as initially prepared in the displaced thermal state with an amplitude of displacement equal to the parameter β used earlier.

The degree of macroscopicity of the state of the mechanical mode after homodyne detection is plotted against the cavity damping rate in figure 8. Indeed, the macroscopic quantumness of the state is much less than when the mirror was initially in a coherent state. In this case, there is never a point where the macroscopic quantumness is close to the upper bound provided by the mean number of excitations in the mechanical state.

Instances of the shape taken by the Wigner function of the mechanical system as κ increases are given in figure 9, which illustrates well the causes of the decreased value of $\mathcal{I}$: the Gaussian peaks representing the distinguishable components in the cat-like state engineered by our conditional approach are made to merge by the increasing damping mechanism, while the interference fringes become less prominent. We can still see negativity in the Wigner function for κ/ω_m up to 0.5, thus demonstrating a residual quantum nature of the corresponding state. However both the amplitude and the frequency of the fringes are depleted, thus resulting in lower values of $\mathcal{I}$.

5. Macroscopicity of excitation-subtracted mechanical states

In this Section we address another class of non-classical states achieved by conditioning the mechanical part of an optomechanical system by means of measurements performed on the cavity field. Specifically, we consider the reduced mechanical states achieved by subtracting one photon from the field, thus following the scheme proposed in reference [38] and developed further in [39]. Such a scheme is able to generate non-classical states of the mechanical mode that, under suitable operating conditions, exhibit a pronounced

Figure 9. Wigner functions of the time evolved state of the mirror from an initial thermal state when $\kappa/\omega_m = 0.02, 0.1, 0.2$ and 0.5, respectively.

cat-like form while resembling a single-excitation number state at low temperature and for a low-mass mechanical mode.

While we refer to references [38, 39] for details on the protocol itself, it is sufficient to mention here that the conditional state ρ_{ps} of the mechanical system achieved upon subjecting the cavity field to the subtraction of a single photon can be written as

$$\rho_{ps} = \frac{\mathcal{N}}{\pi^2} \int \chi'(\gamma) D(-\gamma) d^2\gamma \tag{23}$$

with $\mathcal{N}$ a normalization constant and $\chi'(\gamma)$ the characteristic function of the reduced state of the mechanical system, conditioned on the subtraction of a single quantum from the state of the field. Its form is immaterial for the scopes of this manuscript and can be retrieved from references. [38, 39]. The Wigner function corresponding to such state is readily cast in the form

$$W_{ps}(\delta) = \mathcal{N}\mathcal{A}(\delta)e^{-2\delta\sigma^{-1}\delta^T} \tag{24}$$

with $\delta = (\text{Re}(\delta), \text{Im}(\delta))$ the vector of phase-space variables, $\sigma = \text{diag}[(\Delta x)^2, (\Delta p)^2]$ the matrix of variances of the quadrature operators of the mechanical mode, and $\mathcal{A}(\delta)$ a second-degree polynomial of variable δ. Depending on the parameters of the problem, $\mathcal{A}(\delta)$ can take negative values in certain regions of the phase space, thus leading to the possibility to enforce mechanical non-classicality through photon subtraction.
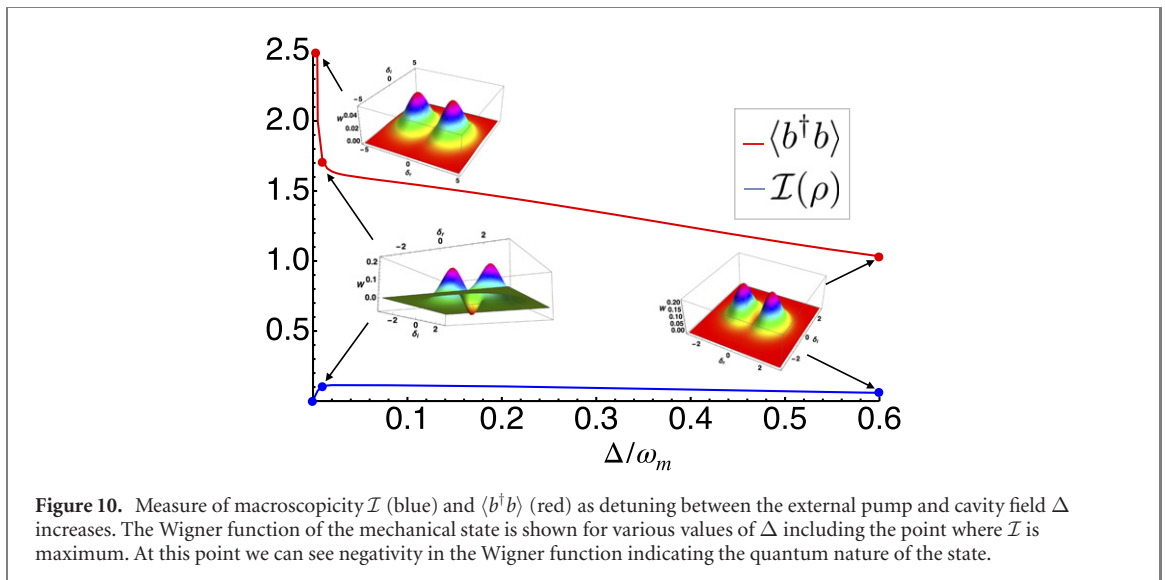
The evaluation of the measure of macroscopic quantumness is then performed using the alternative expression for $\mathcal{I}(\rho)$ given in reference [19]

$$\mathcal{I}(\rho_{ps}) = -\frac{\pi}{2} \int d^2\delta\, W_{ps}(\delta) \partial^2_{\delta\delta*} W_{ps}(\delta), \tag{25}$$

while the evaluation of the mean number of excitations in the state of the mechanical mode makes use of the expression

$$\langle b^\dagger b \rangle = \int |\delta|^2 W_{ps}(\delta) d^2\delta - \frac{1}{2}, \tag{26}$$

which can be easily proven following reference. [33] and the lines sketched in the appendix. The results of our analysis are reported in figure 10, where we study the measure of macroscopicity against the detuning Δ between external pump and cavity field in relation to the Wigner function of the mechanical mode. There is clearly a working point—corresponding to small values of Δ with respect to the cavity frequency—at which the mechanical mode achieves the largest macroscopic quantumness allowed by the conditions of its dynamics, although such value is far from being the maximum possible one, as it can be appreciated by comparing $\mathcal{I}(\rho_{ps})$ to the red curve in figure 10, which shows the mean number of excitations in the reduced mechanical state. Such a discrepancy is easily justified by the fact that the initial state of the mechanical system considered in this analysis is mixed.

Figure 10. Measure of macroscopicity $\mathcal{I}$ (blue) and $\langle b^\dagger b \rangle$ (red) as detuning between the external pump and cavity field Δ increases. The Wigner function of the mechanical state is shown for various values of Δ including the point where $\mathcal{I}$ is maximum. At this point we can see negativity in the Wigner function indicating the quantum nature of the state.

6. Conclusions

We have studied the relative performance of conditional measurements that can be made on a cavity field in an optomechanical system to engineer macroscopic quantum states of a mechanical mode. We focused on the influence that the measurement settings of general homodyne and heterodyne measurements performed on the light field of an optomechanical system have on the degree of macroscopicity of the mechanical state. Both classes of Gaussian measurements are successful in generating macroscopic quantum states, steering the mechanical mode toward states that strongly resemble Schrödinger cat states. However, qualitatively significant differences emerge from different choices of general-dyne measurements performed on the light field, showing that the specific conditional choice to apply in order to generate a macroscopically quantum state should be gauged against the operating conditions of the optomechanical system. Furthermore, the quantum nature of the state persists even in the presence of dissipative processes, making the conditional scheme for mechanical macroscopicity robust. Secondly, we studied the effect of a scheme based on photon subtraction on the degree of macroscopic quantumness of the mechanical mode finding working points at which it is possible to generate a mechanical state exhibiting macroscopic quantum features, although the degree of macroscopic quantumness remains comparatively low. Our study, which is based on a general optomechanical system (cf equation (1)), provides results that are relevant for a range of different experimental settings [4], including cavity-less platforms where the ability to reconstruct quasi-probability functions has been demonstrated [40].

Acknowledgments

Appendix A. Linearized dynamics

The main focus of our study is on systems with cubic optomechanical interactions as described by the Hamiltonian in equation (1). In this appendix, we address linearized dynamics with interaction Hamiltonians of the form

$$H_{\text{lin}} = -\hbar g \sqrt{\bar{n}_{\text{cav}}}(\delta a^\dagger + \delta a)(b + b^\dagger), \tag{27}$$

where $n_{\text{cav}} = \langle a^\dagger a \rangle$ is the average number of photons. When the initial optical state is Gaussian, the evolved mechanical mode would be in a Gaussian state. This state would remain Gaussian under optical general-dyne measurements.

However, this does not mean that the mechanical state could not be described as macroscopically quantum. In fact, using the measure of macroscopic quantumness in reference [19], some Gaussian states, such as squeezed states, can achieve a nonzero value for macroscopicity. This may seem surprising as

Gaussian states lack negativity or interference fringes. It is explained in reference [19] that compressing the Wigner function results in large frequency components and this leads to nonzero values of $\mathcal{I}(\rho)$.

For a single-mode Gaussian state, macroscopicity is straightforward to calculate as shown in reference [19]. Writing its characteristic function as

$$\chi(\xi) = \exp[-A\xi_r^2/2 - B\xi_i^2/2], \tag{28}$$

where A and B are real and positive such that $AB \geqslant 1$, the value of the measure is given by

$$\mathcal{I}(\rho) = (A + B - 2AB)/[4(AB)^{3/2}]. \tag{29}$$

In the case of pure states, when $AB = 1$, the more the state is squeezed, the higher its macroscopicity.

Even though macroscopic quantumness can be found in the linearized interaction case, our study remains centered on systems with dynamics in equation (1). This dynamics produces superposition states and states with Wigner negativity which are more commonly associated with macroscopicity.

Appendix B. Relation between Wigner function and mean number of excitations

Here we provide details on the calculation of the expression in equation (26), which can be deduced from the calculation of the Wigner function of operator $b^\dagger b$ and the use of the trace rule in phase space. We start from equation (23), from which we have

$$\langle b^\dagger b \rangle = \frac{\mathcal{N}}{\pi^2} \int \chi'(\gamma) \, \mathrm{Tr}[b^\dagger b D(-\gamma)] \mathrm{d}^2\gamma. \tag{30}$$

The trace within the integral can be evaluated using the cyclic property of trace, the commutation relation $[b, b^\dagger] = \mathbb{1}$ and the over-complete basis of coherent states as follows

$$\mathrm{Tr}[b^\dagger b D(-\gamma)] \equiv \mathrm{Tr}[b^\dagger D(-\gamma) b] - \mathrm{Tr}[D(-\gamma)]$$

$$= \mathrm{Tr}[b^\dagger D(-\gamma) b] - \pi\delta^2(-\gamma)$$

$$= \frac{1}{\pi} \int |\beta|^2 \, e^{-|\gamma|^2/2 + \gamma^*\beta - \gamma\beta^*} \, \mathrm{d}^2\beta - \pi\delta^2(-\gamma). \tag{31}$$

When used in equation (30) with $\chi'(\gamma)$ replaced by the anti-Fourier transform of the Wigner function $W_{\mathrm{ps}}(\delta)$, one finds equation (26).

ORCID iDs

Hannah McAleese ⬤ https://orcid.org/0000-0003-1016-5952
Mauro Paternostro ⬤ https://orcid.org/0000-0001-8870-9134

References

[1] Schrödinger E 1935 *Die Naturwissenschaften* **23** 807
[2] Zurek W H 2003 arXiv:quant-ph/0306072
[3] Fröwis F, Sekatski P, Dür W, Gisin N and Sangourd N 2018 *Rev. Mod. Phys.* **90** 025004
[4] Aspelmeyer M, Kippenberg T J and Marquardt F 2014 *Rev. Mod. Phys.* **86** 1391
[5] Bose S, Jacobs K and Knight P L 1997 *Phys. Rev. A* **56** 4175
[6] Bose S, Jacobs K and Knight P L 1999 *Phys. Rev. A* **59** 3204
[7] Marshall W, Simon C, Penrose R and Bouwmeester D 2003 *Phys. Rev. Lett.* **91** 130401
[8] Kleckner D, Pikovski I, Jeffrey E, Ament L, Eliel E, van den Brink J and Bouwmeester D 2008 *New J. Phys.* **10** 095020
[9] Li J, Gröblacher S and Paternostro M 2013 *New J. Phys.* **15** 033023
[10] Carlisle A, Kwon H, Jeong H, Ferraro A and Paternostro M 2015 *Phys. Rev. A* **92** 022123
[11] Leggett A J 1980 *Prog. Theor. Phys. Suppl.* **69** 80
[12] Leggett A J 2002 *J. Phys.: Condens. Matter* **14** R415
[13] Dür W, Simon C and Cirac J I 2002 *Phys. Rev. Lett.* **89** 210402
[14] Shimizu A and Miyadera T 2002 *Phys. Rev. Lett.* **89** 270403
[15] Björk G and Mana P G L 2004 *J. Opt. B: Quantum Semiclass. Opt* **6** 429
[16] Cavalcanti E G and Reid M D 2006 *Phys. Rev. Lett.* **97** 170405
[17] Cavalcanti E G and Reid M D 2008 *Phys. Rev. A* **77** 062108
[18] Marquardt F, Abel B and von Delft J 2008 *Phys. Rev. A* **78** 012109
[19] Lee C-W and Jeong H 2011 *Phys. Rev. Lett.* **106** 220401
[20] Park C-Y and Jeong H 2016 arXiv:1606.07213
[21] Fröwis F and Dür W 2012 *New J. Phys.* **14** 093039

[22] Nimmrichter S and Hornberger K 2013 *Phys. Rev. Lett.* **110** 160403
[23] Sekatski P, Sangourd N and Gisin N 2014 *Phys. Rev.* A **89** 012116
[24] Sekatski P, Yadin B, Renou M-O, Dür W, Gisin N and Fröwis F 2018 *New J. Phys.* **20** 013025
[25] Laghaout A, Neergard-Nielsen J S and Andersen U L 2015 *Opt. Commun.* **337** 96
[26] Yadin B and Vedral V 2015 *Phys. Rev.* A **92** 022356
[27] Kwon H, Park C-Y, Tan K C and Jeong H 2017 *New J. Phys.* **19** 043024
[28] Schrinski B, Nimmrichter S, Stickler B A and Hornberger K 2019 *Phys. Rev.* A **100** 032111
[29] Pirkkalainen J M, Cho S U, Massel F, Tuorila J, Heikkilä T T, Hakonen P and Sillanpää M 2015 *Nat. Commun.* **6** 6981
[30] Meenehan S M, Cohen J D, Gröblacher S, Hill J T, Safavi-Naeini A H, Aspelmeyer O and Painter M 2014 *Phys. Rev.* A **90** 011803
[31] Vanner M R, Pikovski I, Cole G D, Kim M S, Brukner C, Hammerer K, Milburn G J and Aspelmeyer M 2011 *Proc. Natl Acad. Sci.* **108** 16182
[32] Rossi M, Mason D, Chen J and Schliesser A 2019 *Phys. Rev. Lett.* **123** 163601
[33] Ferraro A, Olivares S and Paris M G A 2005 Gaussian states in continuous variable quantum information (arXiv:quant-ph/0503237)
[34] Jeong H, Kang M and Kwon H 2015 *Opt. Commun.* **337** 12
[35] Vanner M R, Hofer J, Cole G D and Aspelmeyer M 2013 *Nat. Commun.* **4** 2295
[36] Dall'Arno M, D'Ariano G M and Sacchi M F 2010 *Phys. Rev.* A **82** 042315
[37] Dalibard J, Castin Y and Mølmer K 1992 *Phys. Rev. Lett.* **68** 580
[38] Paternostro M 2011 *Phys. Rev. Lett.* **106** 183601
[39] Khan M M, Akram M J, Paternostro M and Saif F 2016 *Phys. Rev.* A **94** 063830
[40] Rashid M, Toroš M and Ulbricht H 2017 *Quant. Measur. Quant. Metrol.* **4** 17